

LETTERS

Phosphatidylserine-dependent engulfment by macrophages of nuclei from erythroid precursor cells

Hideyuki Yoshida¹, Kohki Kawane^{1,3,4}, Masato Koike², Yoshimi Mori⁵, Yasuo Uchiyama² & Shigekazu Nagata^{1,3,4}

Definitive erythropoiesis usually occurs in the bone marrow or fetal liver, where erythroblasts are associated with a central macrophage in anatomical units called 'blood islands'^{1,2}. Late in erythropoiesis, nuclei are expelled from the erythroid precursor cells and engulfed by the macrophages in the blood island^{2,3}. Here we show that the nuclei are engulfed by macrophages only after they are disconnected from reticulocytes, and that phosphatidylserine, which is often used as an 'eat me' signal for apoptotic cells, is also used for the engulfment of nuclei expelled from erythroblasts. We investigated the mechanism behind the enucleation and engulfment processes by isolating late-stage erythroblasts from the spleens of phlebotomized mice. When these erythroblasts were cultured, the nuclei protruded spontaneously from the erythroblasts. A weak physical force could disconnect the nuclei from the reticulocytes. The released nuclei contained an undetectable level of ATP, and quickly exposed phosphatidylserine on their surface. Fetal liver macrophages efficiently engulfed the nuclei; masking the phosphatidylserine on the nuclei with the dominant-negative form of milk-fat-globule EGF8 (MFG-E8) prevented this engulfment.

Phlebotomy promotes the development of erythroid cells in mouse spleen^{4,5}. We used this system to obtain a large number of erythroblasts at a synchronized developmental stage. When prepared from spleens 4 days after phlebotomy, about 60% of the purified erythroblasts were CD71⁺Ter119⁺ (Fig. 1a). Few CD117(c-Kit)⁺ cells were present, indicating that the cells were erythroblasts at the late stage of erythropoiesis (Fig. 1b)⁶. When the erythroblasts were cultured at 37 °C, some cells started blebbing and the nucleus moved to one side of the cell (Supplementary Movie 1). After 5 h, about 12% of the erythroblasts possessed an eccentric nucleus that could be distinguished from the irregularly shaped reticulocytes (Fig. 1c). Observation by electron microscopy indicated that the nucleus was surrounded by an intact plasma membrane and was connected to the reticulocytes by means of a thin pseudopodium-like membrane extension (Fig. 1d). After collection and resuspension of the enucleating erythroblasts, most nuclei became disconnected from the reticulocytes, indicating that the connection between the nucleus and reticulocyte could be disrupted by weak physical stress. In fact, many nuclei could be disconnected from reticulocytes by gently pipetting the erythroblasts in and out five times.

We then monitored the enucleation process with two different DNA-staining dyes, SYTO16 and SYTOX blue, which are cell-permeable and cell-impermeable fluorescent dyes, respectively. Erythroblasts were represented by a population (P6) of high forward scatter (FSC) with SYTO16^{high} SYTOX⁻ (Fig. 2a). The cells with low FSC (FSC^{low}) consist of two populations, the expelled nuclei, which were SYTO16^{high} SYTOX⁻ (P3), and SYTO16^{low} SYTOX⁻ reticulocytes (P4). All SYTOX⁺ cells were dead. When the erythroblasts were

incubated at 37 °C, their number did not change significantly (Fig. 2b). There were no free nuclei before incubation, but their number increased gradually during incubation. This increase paralleled an increase in reticulocyte numbers. Because the extruded

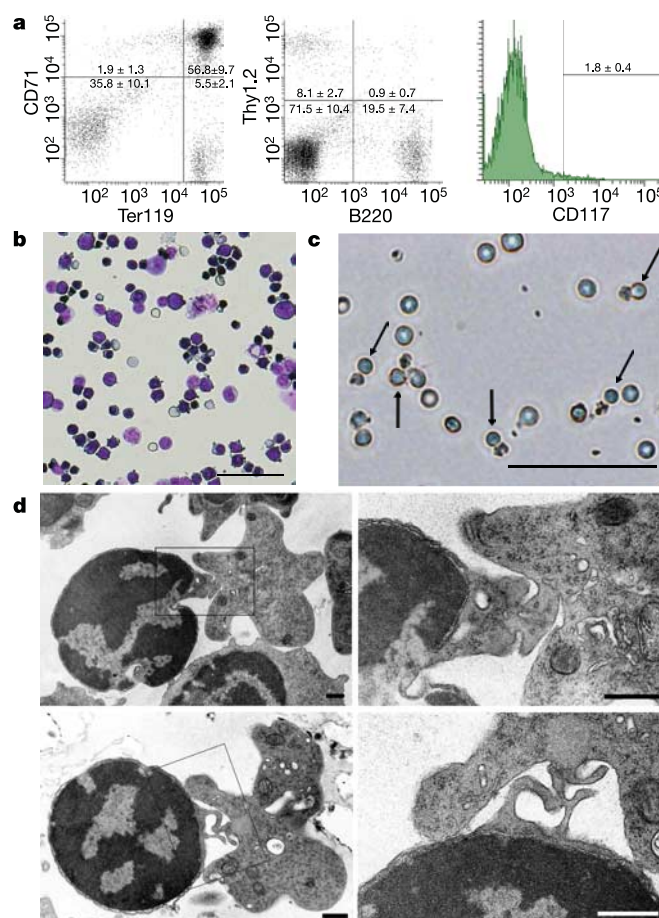


Figure 1 | Enucleation of erythroblasts. **a**, Erythroblasts from phlebotomized mice were stained for Ter119 and CD71, or B220 and Thy 1.2, and analysed by flow cytometry. Numbers indicate the percentage of stained cells in each quadrant. Experiments were performed three times, and the numerical results shown are means ± s.d. The staining profile for CD117 (c-Kit) is also shown. **b**, Erythroblasts stained with Wright-Giemsa. Scale bar, 50 μm. **c**, Erythroblasts incubated for 5 h. Nuclei protruding from erythroblasts are indicated by arrows. Scale bar, 50 μm. **d**, Electron microscopy of erythroblasts incubated for 3 h. Boxed areas in the left panels are enlarged in the right panels. Scale bar, 1 μm.

¹Department of Genetics and ²Department of Cell Biology and Neuroscience, Graduate School of Medicine, Osaka University, Osaka 565-0871, Japan. ³Laboratory of Genetics, Integrated Biology Laboratories, Graduate School of Frontier Biosciences, Osaka University, Osaka 565-0871, Japan. ⁴Core Research for Evolutional Science and Technology, Japan Science and Technology Corporation, Osaka 565-0871, Japan. ⁵Sakura Motion Picture Co. Ltd, 20-1 Sendagaya 4-chome, Shibuya, Tokyo 151-0051, Japan.

nuclei were connected to the reticulocytes before this procedure, it is likely that the FACS procedure, which includes the centrifugation and suspension of cells, disconnected the extruded nuclei from the reticulocytes. In accord with a previous report⁷, the production of reticulocytes and the release of nuclei were inhibited by $10 \mu\text{g ml}^{-1}$ cytochalasin B (Fig. 2b), indicating that actin polymerization is involved in the enucleation process. Erythropoietin is indispensable for definitive erythropoiesis⁸. However, in accord with the report that the erythropoietin receptor is downregulated at early stages of erythropoiesis⁹, erythropoietin had no effect on the enucleation process (Fig. 2b). The involvement of caspase in erythroid cell differentiation has been suggested^{10,11}. But, the enucleation process described above was not prevented by caspase inhibitors (benzyloxy-carbonyl-VAD) at $100 \mu\text{M}$ (data not shown), and there was no apoptotic DNA degradation in the nuclei expelled from the erythroid precursor cells (Fig. 2c).

Apoptotic cells expose phosphatidylserine (PtdSer) on their surface as a signal for macrophages to engulf them¹². We examined whether the nuclei might also use PtdSer to be recognized by macrophages. Erythroblasts were cultured for 3 h to allow the enucleation process to begin, then stained with SYTO16, SYTOX and Cy5-labelled Annexin V and analysed by three-colour flow cytometry. As shown in Fig. 3a, nucleated erythroblasts and reticulocytes were Annexin V⁻, whereas SYTOX⁺ dead cells were Annexin V⁺. The nuclei were also Annexin V⁻. However, when the cultures

were subjected to weak physical stress and then incubated further, the nuclei became Annexin V⁺. In contrast, the reticulocytes and erythroblasts remained Annexin V⁻ after the physical stress. The Annexin V⁺ nuclei remained SYTOX⁻, indicating that the plasma membrane surrounding the nuclei remained intact after the physical stress. The exposure of PtdSer on the expelled nuclei was also observed with erythroblasts prepared from fetal liver. To further confirm the exposure of PtdSer, the erythroblasts were labelled with biotin-labelled Annexin V, followed by staining with gold-conjugated streptavidin. As shown in Fig. 3b, no gold particles were found on the nuclei protruding from reticulocytes, whereas gold labelling was observed on the outer leaflet of the continuous plasma membrane of the nuclei that were disconnected from reticulocytes. These results indicated that the nuclei exposed PtdSer only after they had been disconnected from the reticulocytes. PtdSer is normally confined to the inner leaflet of the plasma membrane¹³. This asymmetry is maintained by a combination of an ATP-dependent aminophospholipid translocase that specifically transports PtdSer from the outer to the inner leaflet of the plasma membrane, and a Ca²⁺-dependent but energy-independent scramblase that non-specifically randomizes lipids across the bilayer. As shown in Fig. 3c, the ATP level was decreased to undetectability in the nuclei expelled from reticulocytes, whereas the Ca²⁺ level was much higher in the nuclei than in the reticulocytes (Fig. 3d, e).

Nuclei released from erythroblasts were then isolated by a cell

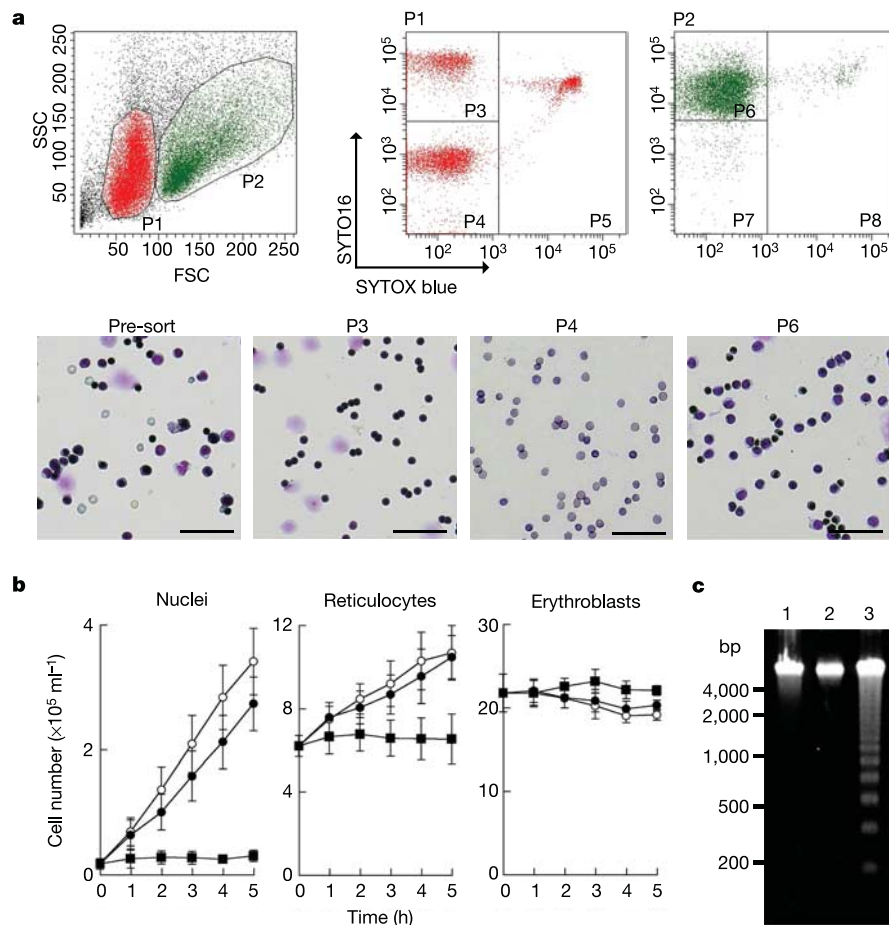


Figure 2 | Flow cytometric analysis of enucleation. **a**, Erythroblasts incubated for 5 h were stained with SYTO16 and SYTOX, then analysed by flow cytometry. Top left, a plot of side light scatter (SSC) against forward light scatter (FSC), from which events in P1 (top middle) and P2 (top right) are shown for SYTO16 and SYTOX. Bottom, cells in each fraction were stained with Wright-Giemsa. **b**, Erythroblasts were incubated with no additions (open circles), 2 units ml^{-1} erythropoietin (filled circles) or

2 units ml^{-1} erythropoietin and $10 \mu\text{g ml}^{-1}$ cytochalasin B (squares). Experiments were performed twice in triplicate; results are means \pm s.d. **c**, Erythroblasts were cultured for 5 h in the absence (lane 1) or presence (lane 2) of erythropoietin. Nuclei were collected, and DNA was subjected to electrophoresis on an agarose gel. As a control, DNA from SYTOX⁺ cells (lane 3) was analysed. bp, base pairs.

sorter and used as prey for macrophages. We used macrophages from the liver of DNase II^{-/-} embryos as phagocytes to reveal the engulfed nuclei clearly¹⁴. As shown in Fig. 4a and Supplementary Movies 2 and 3, macrophages efficiently engulfed nuclei, and the phagocytosis index (the number of engulfed nuclei per macrophage) was 2.4 after incubation for 2 h (Fig. 4b). MFG-E8 binds PtdSer through its Factor VIII-homologous domains at the carboxy terminus, whereas it binds macrophages through its RGD motif at the amino terminus¹⁵. A point

mutant (D89E) of MFG-E8 in the RGD motif binds PtdSer exposed on apoptotic cells, and inhibits their engulfment by macrophages¹⁵. Similarly, the D89E mutant dose-dependently inhibited the engulfment of nuclei by macrophages, and the phagocytosis index decreased to less than 0.05 in the presence of 64 ng ml⁻¹ D89E mutant (Fig. 4b). These results indicated that PtdSer exposed on the expelled nuclei was required for their engulfment by macrophages.

Proliferating erythroblasts are closely associated with macro-

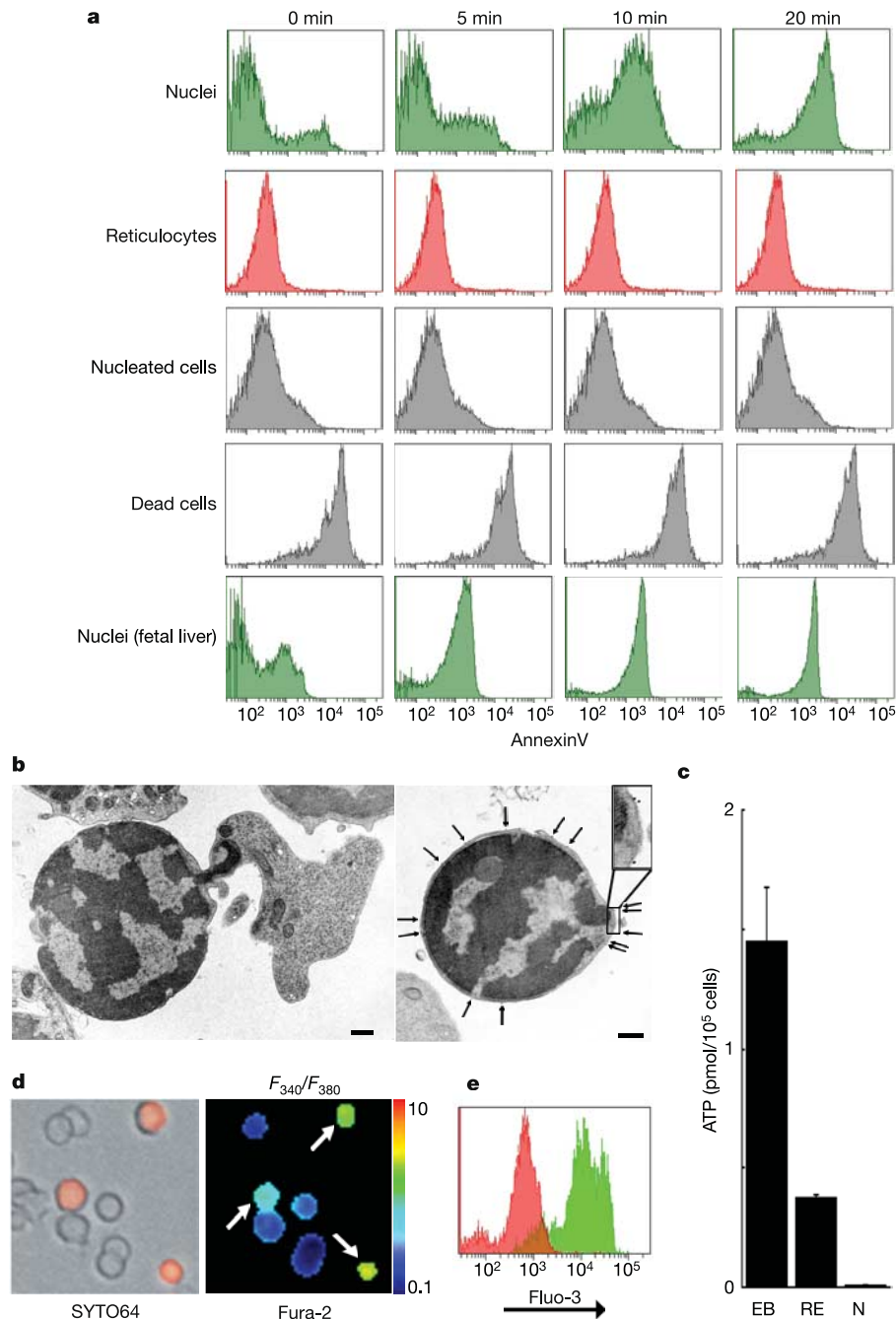


Figure 3 | Exposure of PtdSer on nuclei released from erythroblasts.

a, Erythroblasts from the spleens of phlebotomized mice were cultured for 3 h, pipetted in and out five times, and incubated further for the indicated periods. The Annexin V staining profiles for nuclei, reticulocytes, erythroblasts and dead cells are shown. The nuclei from fetal liver erythroblasts were also examined. **b**, Erythroblasts incubated for 3 h were labelled with biotin–Annexin V, followed by staining with streptavidin-conjugated colloidal gold, and analysed by electron microscopy. Scale bar, 1 μ m. Arrows indicate gold particles on plasma membranes. An enlarged

image of the boxed area is shown at top right. **c**, ATP levels for erythroblasts (EB), reticulocytes (RE) and nuclei (N). Experiments were performed twice in duplicate; results are means + s.d. **d**, Right, erythroblasts were loaded with Fura-2. The scale at the right shows the reference image for F_{340}/F_{380} . High F_{340}/F_{380} ratios reflect high intracellular Ca^{2+} concentrations. Left, cells were stained for nuclei (red). **e**, Erythroblasts were loaded with Fluo-3 and stained with SYTO64 and SYTOX. Fluorescence-activated cell-sorting profiles for Fluo-3 in SYTO64^{low}SYTOX⁻ (reticulocytes, red) and in SYTO64^{high}SYTOX⁻ (nuclei, green) are shown.

phages in the blood islands until the nuclei are expelled, and several molecules, including cadherin, integrins and a 30-kDa protein, have been proposed to participate in the interaction between erythroblasts and macrophages¹⁶. Here we showed that the nucleus spontaneously protruded from erythroblasts, remaining connected by means of a thin membrane extension, and a weak physical force could disconnect the nucleus from the reticulocyte. Cells in blood islands are exposed to shear stress, the tangential component of haemodynamic forces¹⁷. When erythroblasts undergo enucleation, the membrane composition changes between the reticulocytes and the nuclei, with the plasma membrane surrounding the extruding nuclei becoming enriched in a receptor for concanavalin A or the binding site for merocyanine 540 (refs 18, 19). Probably as a result of such changes, the reticulocytes lose their affinity for the macrophages, whereas the nuclei remain attached to the macrophages. The exposure of erythroblasts carrying protruded nuclei to shear stress might be sufficient to release the reticulocytes physically from the nuclei and into the bloodstream.

Using the finding that protruding nuclei are disconnected from reticulocytes by weak physical stress, we showed that the expelled nuclei expose PtdSer only after they have been disconnected from the reticulocytes. The extruded nuclei contained an extremely low level of ATP. Because the nuclei contain little cytoplasm, it is likely that ATP is not supplied in the nuclei. In return, the Ca^{2+} concentration increased in the nuclei, probably as a result of inactivation of the plasma membrane Ca^{2+} ATPase, which pumps Ca^{2+} against its large concentration gradient out of the cells in an ATP-dependent manner²⁰. Thus, the aminophospholipid translocase is inactivated, whereas scramblase is activated, causing the exposure of PtdSer on the surface of nuclei. The putative aminophospholipid translocase and several scramblases have been identified^{21,22}. However, the involvement of these molecules in exposing PtdSer on the outer leaflet during apoptosis has not been proven^{23,24}. The rapid exposure of PtdSer on the nuclei expelled from erythroblasts might help in elucidating the molecular mechanism by which the asymmetrical distribution of phospholipids is maintained in the plasma membrane.

Masking PtdSer on apoptotic cells inhibits their engulfment by macrophages^{15,25,26}. Similarly, engulfment of the expelled erythroid nuclei was inhibited by the dominant-negative form of MFG-E8, indicating that PtdSer exposed on the nucleus surface works as an 'eat nucleus' signal. Several molecules expressed in macrophages have been proposed to bind PtdSer for the engulfment of apoptotic cells^{15,26,27}. Among them, MFG-E8 is expressed by thiolglycollate-elicited peritoneal macrophages, immature dendritic cells and tingible-body macrophages in the spleen. However, it is not expressed in fetal liver macrophages or bone marrow macrophages²⁸. Accordingly, fetal liver macrophages from MFG-E8^{-/-} embryos engulfed the

nuclei as efficiently as wild-type fetal liver macrophages did (data not shown). It remains to be shown whether any other molecules that are proposed to participate in the engulfment of apoptotic cells are involved in the engulfment of expelled nuclei. We recently reported that the systemic administration of the dominant-negative MFG-E8 induces autoimmunity in mice by inducing the production of anti-nuclear and anti-phosphatidylserine antibodies²⁹. We thought that this was due to blockage of the engulfment of apoptotic cells. However, the adult human produces 2×10^{11} erythrocytes per day, indicating that blockage of the engulfment of nuclei might also contribute to the development of autoimmunity.

METHODS

Mice and materials. C57BL/6J mice were purchased from Charles River Japan. DNase II^{-/-} mice were described previously³. All mice were housed in a specific pathogen-free facility at Osaka University Medical School, and all animal experiments were performed in accordance with protocols approved by the Osaka University Medical School Animal Care and Use Committee.

Human erythropoietin was from Kirin Brewery and transferrin was from Sigma. The D89E mutant of mouse MFG-E8 was prepared as described¹⁵. Phycoerythrin (PE)-conjugated or fluorescein isothiocyanate (FITC)-conjugated monoclonal antibodies against Ter119, CD71, c-Kit, Thy1.2 and B220 were from BD Biosciences. Indodicarbocyanine (Cy5)-conjugated and biotin-conjugated Annexin V were from BioVision. SYTO16, SYTO64 and SYTOX were from Molecular Probes.

Preparation of erythroblasts and macrophages. Blood samples (0.5 ml) were withdrawn from ten-week-old female mice by venipuncture; four days later, erythroblasts were prepared from the mice's spleens. Erythroblasts were also prepared from fetal livers at embryonic day 13.5 (E13.5). The cell suspension was passed through a mesh, layered onto a density gradient of 70% (v/v) Percoll (Amersham Biosciences) and centrifuged at 400g for 30 min. Erythroblasts were collected and suspended in α -minimal essential medium (α -MEM) containing 10% FCS. Erythroblasts were characterized by staining with $0.25 \mu\text{g ml}^{-1}$ PE-anti-Ter119, $2.5 \mu\text{g ml}^{-1}$ FITC-anti-CD71, $1.25 \mu\text{g ml}^{-1}$ FITC-anti-Thy1.2, $0.5 \mu\text{g ml}^{-1}$ PE-anti-B220 or $5 \mu\text{g ml}^{-1}$ FITC-anti-CD117, followed by flow cytometry with a FACSAria cell sorter (BD Biosciences).

To prepare fetal liver macrophages, livers from E14.5 DNase II^{-/-} embryos were minced, incubated at 37°C for 5 min in perfusion medium (Invitrogen) and then for 40 min in digestion medium (Invitrogen). The cells were passed through a mesh and cultured in α -MEM containing 10% FCS and mouse macrophage colony-stimulating factor³⁰. After being cultured for 2 weeks the cells expressed F4/80 and were used as fetal liver macrophages.

Enucleation assay. Erythroblasts (3×10^6 cells ml^{-1}) were incubated at 37°C in α -MEM containing 10% FCS and $500 \mu\text{g ml}^{-1}$ transferrin. After incubation, cells were stained at 22°C for 20 min with $0.25 \mu\text{M}$ SYTO16 and $0.2 \mu\text{M}$ SYTOX in 10 mM HEPES buffer pH 7.4 containing 140 mM NaCl and 5 mM MgCl_2 , and analysed by flow cytometry. To detect PtdSer, erythroblasts were stained with Cy5-labelled Annexin V in 10 mM HEPES buffer pH 7.4 containing 140 mM NaCl and 2.5 mM CaCl_2 (binding buffer). After being washed with binding buffer, the cells were further stained with SYTO16 and SYTOX, then analysed by flow cytometry. For cytochemical analysis the cells were cytospun, then stained with Wright-Giemsa.

Assay for intracellular ATP and Ca^{2+} . Erythroblasts (3×10^7 cells) from the spleens of phlebotomized mice were incubated at 37°C for 3 h, and FSC^{high} SYTO16^{high} SYTOX⁻ erythroblasts, FSC^{low} SYTO16^{high} SYTOX⁻ nuclei and FSC^{low} SYTO16^{low/-} SYTOX⁻ reticulocytes were collected with a FACSAria cell sorter. The ATP level was then determined with an ATP Bioluminescence Assay Kit CLSII (Roche) using 10^5 cells or nuclei. For determining the cellular Ca^{2+} level, erythroblasts were treated at 37°C for 30 min with $1.8 \mu\text{M}$ Fluo-3 acetoxymethyl ester or $1 \mu\text{M}$ Fura-2 acetoxymethyl ester (Dojindo) in α -MEM containing 0.02% Pluronic F-127 (Molecular Probes). The cells loaded with Fluo-3 were further stained with $2 \mu\text{M}$ SYTO64 and $0.2 \mu\text{M}$ SYTOX, then analysed by flow cytometry. The Fura-2-loaded cells were irradiated with ultraviolet at 340 nm followed by ultraviolet at 380 nm. Emission fluorescence, F , was recorded on an ORCA-ER charge-coupled device camera (Hamamatsu Photonics) through a Diaphoto 300 fluorescence microscope (Nikon), and the data processed with an AquaCosmos image processor (Hamamatsu Photonics) to obtain the ratio F_{340}/F_{380} .

Engulfment of nuclei by macrophages. To prepare nuclei, 3×10^7 erythroblasts were incubated at 37°C for 5 h and stained with SYTO16 and SYTOX. The nuclei, represented by FSC^{low} SYTO16^{high} SYTOX⁻, were collected with a cell sorter. DNase II^{-/-} fetal liver macrophages (2×10^4 cells) were cultured in

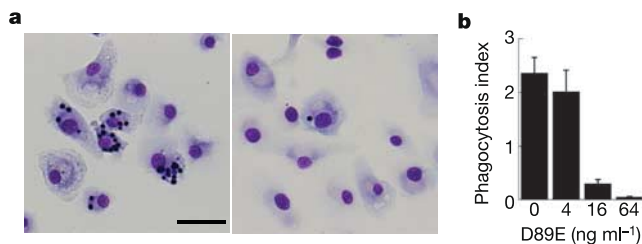


Figure 4 | Phosphatidylserine-dependent engulfment of nuclei. **a**, Fetal liver macrophages were co-cultured with nuclei in the absence (left) or presence (right) of 64 ng ml^{-1} D89E. The cells were then stained with Wright-Giemsa. Scale bar, $50 \mu\text{m}$. **b**, Engulfment of nuclei by fetal liver macrophages was performed in the presence of the indicated concentrations of D89E. The experiments were performed three times; results are values of the phagocytosis index (the number of engulfed nuclei per macrophage) and are shown as means \pm s.d.

α -MEM containing 10% FCS on eight-well Lab-Tek II chamber slides (Nalge Nunc). Nuclei (4×10^5) were added to the macrophages and incubated at 37 °C for 2 h. Unengulfed nuclei were removed by vigorous washing, and the macrophages were stained with Wright-Giemsa.

Electron microscopy. Cells were collected by centrifugation at 500g for 5 min, washed with PBS, fixed with 2% glutaraldehyde, 2% paraformaldehyde in 0.1 M phosphate buffer pH 7.2, postfixed with 1% OsO₄ at 4 °C for 2 h and embedded in Epon 812 as described³. To detect the binding of Annexin V to PtdSer at the ultrastructural level, erythroblasts were incubated with biotin-labelled Annexin V as described above, then fixed with 0.2% glutaraldehyde, 4% paraformaldehyde. After being rinsed with PBS, they were incubated with streptavidin-conjugated 15-nm colloidal gold (British Biocell International), fixed again with 2% glutaraldehyde, 2% paraformaldehyde in 0.1 M phosphate buffer pH 7.2, and embedded in Epon 812. Sections (80 nm) were prepared with a Reichert Ultracut N ultramicrotome (Nissei), stained with lead citrate and uranyl acetate, and observed with a Hitachi H-7100 electron microscope.

Received 29 May; accepted 29 June 2005.

- Bessis, M., Mize, C. & Prenant, M. Erythropoiesis: comparison of *in vivo* and *in vitro* amplification. *Blood Cells* **4**, 155–174 (1978).
- Sadahira, Y. & Mori, M. Role of the macrophage in erythropoiesis. *Pathol. Int.* **49**, 841–848 (1999).
- Kawane, K. *et al.* Requirement of DNase II for definitive erythropoiesis in the mouse fetal liver. *Science* **292**, 1546–1549 (2001).
- Pannaciuoli, I. M. *et al.* Effect of bleeding on *in vivo* and *in vitro* colony-forming hemopoietic cells. *Acta Haematol.* **58**, 27–33 (1977).
- Zhang, D. *et al.* An optimized system for studies of EPO-dependent murine pro-erythroblast development. *Exp. Hematol.* **29**, 1278–1288 (2001).
- Socolovsky, M. *et al.* Ineffective erythropoiesis in Stat5a^{-/-}5b^{-/-} mice due to decreased survival of early erythroblasts. *Blood* **98**, 3261–3273 (2001).
- Repasky, E. A. & Eckert, B. S. The effect of cytochalasin B on the nucleation of erythroid cells *in vitro*. *Cell Tissue Res.* **221**, 85–91 (1981).
- Wu, H., Liu, X., Jaenisch, R. & Lodish, H. F. Generation of committed erythroid BFU-E and CFU-E progenitors does not require erythropoietin or the erythropoietin receptor. *Cell* **83**, 59–67 (1995).
- Broudy, V. C., Lin, N., Brice, M., Nakamoto, B. & Papayannopoulou, T. Erythropoietin receptor characteristics on primary human erythroid cells. *Blood* **77**, 2583–2590 (1991).
- Carlisle, G. W., Smith, D. H. & Wiedmann, M. Caspase-3 has a nonapoptotic function in erythroid maturation. *Blood* **103**, 4310–4316 (2004).
- Zermati, Y. *et al.* Caspase activation is required for terminal erythroid differentiation. *J. Exp. Med.* **193**, 247–254 (2001).
- Fadok, V. A., Bratton, D. L., Frasch, S. C., Warner, M. L. & Henson, P. M. The role of phosphatidylserine in recognition of apoptotic cells by phagocytes. *Cell Death Differ.* **5**, 551–562 (1998).
- Balasubramanian, K. & Schroit, A. J. Aminophospholipid asymmetry: A matter of life and death. *Annu. Rev. Physiol.* **65**, 701–734 (2003).
- Kawane, K. *et al.* Impaired thymic development in mouse embryos deficient in apoptotic DNA degradation. *Nature Immunol.* **4**, 138–144 (2003).
- Hanayama, R. *et al.* Identification of a factor that links apoptotic cells to phagocytes. *Nature* **417**, 182–187 (2002).
- Hanspal, M. Importance of cell–cell interactions in regulation of erythropoiesis. *Curr. Opin. Hematol.* **4**, 142–147 (1997).
- Davies, P. F. Flow-mediated endothelial mechanotransduction. *Physiol. Rev.* **75**, 519–560 (1995).
- Schlegel, R. A., Phelps, B. M., Waggoner, A., Terada, L. & Williamson, P. Binding of merocyanine 540 to normal and leukemic erythroid cells. *Cell* **20**, 321–328 (1980).
- Geiduschek, J. B. & Singer, S. J. Molecular changes in the membranes of mouse erythroid cells accompanying differentiation. *Cell* **16**, 149–163 (1979).
- Strehler, E. E. & Treiman, M. Calcium pumps of plasma membrane and cell interior. *Curr. Mol. Med.* **4**, 323–335 (2004).
- Tang, X., Halleck, M. S., Schlegel, R. A. & Williamson, P. A subfamily of P-type ATPases with aminophospholipid transporting activity. *Science* **272**, 1495–1497 (1996).
- Zhou, Q. *et al.* Molecular cloning of human plasma membrane phospholipid scramblase. A protein mediating transbilayer movement of plasma membrane phospholipids. *J. Biol. Chem.* **272**, 18240–18244 (1997).
- Zhou, Q., Zhao, J., Wiedmer, T. & Sims, P. J. Normal hemostasis but defective hematopoietic response to growth factors in mice deficient in phospholipid scramblase 1. *Blood* **99**, 4030–4038 (2002).
- Williamson, P. & Schlegel, R. A. Hide and seek: the secret identity of the phosphatidylserine receptor. *J. Biol.* **3**, 14 (2004).
- Krahling, S., Callahan, M. K., Williamson, P. & Schlegel, R. A. Exposure of phosphatidylserine is a general feature in the phagocytosis of apoptotic lymphocytes by macrophages. *Cell Death Differ.* **6**, 183–189 (1999).
- Fadok, V. A. *et al.* A receptor for phosphatidylserine-specific clearance of apoptotic cells. *Nature* **405**, 85–90 (2000).
- Kawasaki, Y., Nakagawa, A., Nagaosa, K., Shiratsuchi, A. & Nakanishi, Y. Phosphatidylserine binding of class B scavenger receptor type I, a phagocytosis receptor of testicular Sertoli cells. *J. Biol. Chem.* **277**, 27559–27566 (2002).
- Hanayama, R., Tanaka, M., Miwa, K. & Nagata, S. Expression of developmental endothelial locus-1 in a subset of macrophages for engulfment of apoptotic cells. *J. Immunol.* **172**, 3876–3882 (2004).
- Asano, K. *et al.* Masking of phosphatidylserine inhibits apoptotic cell engulfment and induces autoantibody production in mice. *J. Exp. Med.* **200**, 459–467 (2004).
- Takeshita, S., Kaji, K. & Kudo, A. Identification and characterization of the new osteoclast progenitor with macrophage phenotypes being able to differentiate into mature osteoclasts. *J. Bone Miner. Res.* **15**, 1477–1488 (2000).

Supplementary Information is linked to the online version of the paper at www.nature.com/nature.

Acknowledgements We thank H. Fukuyama for help at the initial stage of this work; H. Suzuki, I. Ito and S. Hanasaki for taking the time-lapse video; T. Yanagida for discussion; and M. Fujii and M. Harayama for secretarial assistance. This work was supported in part by Grants-in-Aid from the Ministry of Education, Science, Sports and Culture in Japan.

Author Contributions H.Y. performed most of the experiments. M.K. carried out the electron microscopy analysis, and Y.M. took the time-lapse video. K.K., Y.U. and S.N. contributed to the data analysis. S.N. was responsible for planning the project.

Author Information Reprints and permissions information is available at npg.nature.com/reprintsandpermissions. The authors declare no competing financial interests. Correspondence and requests for materials should be addressed to S.N. (Nagata@genetic.med.osaka-u.ac.jp).